PAPER • OPEN ACCESS

Effects of N/Si ratio on mechanical properties of amorphous silicon nitride coating

Materials Research Express

PAPER

Effects of N/Si ratio on mechanical properties of amorphous silicon nitride coating

Huasi Zhou[1], **Cecilia Persson**[2], **Wei Xia**[1,*] **and Håkan Engqvist**[1,*]

[1] Division of Applied Materials Science, Department of Materials Science and Engineering, Uppsala University, Uppsala, Sweden
[2] Division of Biomedical Engineering, Department of Materials Science and Engineering, Uppsala University, Uppsala, Sweden
* Authors to whom any correspondence should be addressed.

E-mail: Wei.xia@angstrom.uu.se **and** Håkan.engqvist@angstrom.uu.se

Keywords: silicon nitride coating, LPCVD, Hardness and elastic modulus, friction and wear

Supplementary material for this article is available online

OPEN ACCESS

RECEIVED
11 September 2023

REVISED
9 November 2023

ACCEPTED FOR PUBLICATION
21 November 2023

PUBLISHED
30 November 2023

Abstract

The utilization of silicon nitride coatings has been proposed as an effective method to enhance wear resistance and mitigate the release of metallic ions from biomedical implants. However, the relatively high dissolution rate of low-density coatings remains an obstacle to their implementation. Here, chemical vapour deposition techniques may have advantages over the typically used physical vapour deposition (PVD) methods. Therefore, in this study, silicon nitride coatings were obtained by low-pressure chemical vapor deposition (LPCVD). Since the nitrogen-to-silicon (N/Si) ratio and deposition temperature have been reported as major factors affecting the performance of the coatings, the effects of ammonia (NH_3) to dichlorosilane (SiH_2Cl_2) flow ratio and deposition temperature were systemically investigated in the form of microstructure, mechanical and tribological properties of the coatings. The results revealed that the coatings exhibited a dense structure. As the ammonia flow ratio increased, the surface became smoother, and the hardness and elastic modulus increased and reached the maximum at a flow ratio of 4, giving a hardness of around 27 GPa and an elastic modulus of 290 GPa, respectively. The higher mechanical properties of the coatings deposited at a flow ratio of 4 are attributed to the stronger covalent Si-N bonding, as confirmed by XPS results. However, the coatings deposited at a flow ratio of 2 exhibited the lowest wear rate, at 9.5×10^{-7} mm^3 Nm^{-1}, around one-third of the value of the coatings deposited at a flow ratio of 6, likely due to the high silicon content of these coatings. Increasing the temperature resulted in an increased deposition rate, higher hardness and elastic modulus as well as a lower wear rate, likely due to incomplete reactions at lower temperatures. The generally high hardness and low wear rate indicate that the coatings deposited by LPCVD are promising for application in spinal implants.

1. Introduction

Chronic low back pain is one of the most common diseases in adults, mainly caused by degenerative and intervertebral disc diseases [1]. Total disc replacement (TDR), which involves replacing the degenerative disc with an artificial disc made of metal and polymer, is regarded as an effective solution for some patients, enabling a maintenance of the movement of adjacent segments and the patient's long-term remission [1, 2]. Although success rates of up to 80% after 2 years of implantation have been reported, the survival rates decrease significantly after 10 years, which is believed to be due to stress shielding and/or micromotion and ions and wear particles being released from the implant [3]. These ions and wear debris could trigger an inflammatory response, leading to local bone resorption [4]. One solution to this problem could be depositing a coating on the implant as it could act as a barrier to metal ion release [5].

Many ceramic coatings have been extensively studied for the metal part of implants, including graphitic carbon (GLC), chromium nitrides (CrN), diamond-like carbon (DLC), zirconium nitride (ZrN) and silicon

Table 1. Deposition parameters of the coatings.

Coating	Temperature (°C)	Flow ratio (NH_3/DCS)	DCS flow rate (sccm)	NH_3 flow rate (sccm)
Flow ratio = 2	790	2	42	83
Flow ratio = 3	790	3	31	94
Flow ratio = 4	790	4	25	100
Flow ratio = 5	790	5	21	104
Flow ratio = 6	790	6	18	107
T640	640	4	25	100
T690	690	4	25	100

nitride (Si_3N_4) [6]. Among them, Si_3N_4 could be considered one of the most promising candidates for articulating bearing surfaces because of its excellent mechanical (with a coating hardness of around 13–25 GPa) and tribological properties [7, 8]. Moreover, its biological properties also make it unique compared to other ceramic coatings. Silicon nitride wear particles have been found to dissolve in aqueous solutions at a dissolution rate of 0.2–1.4 nm day^{-1} [9, 10], indicating that the negative biological responses resulting from other wear particles could be avoided, and thereby increase the lifetime of the implant, in particular in light of the potential antibacterial properties found in several studies on silicon nitride [11].

In one of our previous studies, Filho *et al* investigated the influence of bias voltage and substrate rotation on the performance of silicon nitride coatings deposited by reactive high-power impulse magnetron sputtering (rHiPIMS) [12]. Based on the results that 1-fold rotation exhibited higher density, the effect of coating density and additional alloying elements (Cr, Nb) on the tribological and corrosion properties of the coatings were further explored and found that while the coatings with higher density exhibited better tribological performance, there was no relationship between the alloy compositions investigated and their wear resistance [13, 14]. In order to further investigate the effect of alloying elements, Skjöldebrand *et al* evaluated compositional gradients of Si-Fe-C-N coatings, finding that the mechanical properties decreased with increasing Fe content but that the coatings showed good biocompatibility with pre-osteogenic MC3T3 cells adhering to the coatings [15]. These studies indicated that the silicon nitride coatings warranted further investigation for use on joint-bearing surfaces. However, some challenges remain. For example, silicon nitride coatings deposited by rHiPIMS have a low density for 3-dimensional structures (when substrate rotation is applied) and low N/Si ratios (0.8–1.15), which results in poor bio-tribological properties, including a high dissolution rate [9].

In order to improve the performance of silicon nitride coatings, another deposition technique - low pressure chemical vapor deposition (LPCVD) - was explored in this study. Compared with rHiPIMS-deposited coatings, LPCVD-deposited coatings exhibit higher uniformity and density since the gaseous precursors are homogeneously filled into the chamber, which is heated uniformly, thus ensuring a uniform process of mass transport and diffusion and the formation of uniform coatings [16]. Additionally, the mean free path of the gas molecules will increase at low deposition pressure, meaning that the unwanted gas reactions decrease [17]. While there are studies on the optimization of properties of LPCVD-deposited silicon nitride coatings [18, 19], a systematic study of the effect of deposition parameters on the mechanical and tribological behavior is lacking. Such knowledge is crucial for a future potential application of silicon nitride coatings to spinal implants.

In this work, silicon nitride coatings were deposited by LPCVD techniques using SiH_2Cl_2 and NH_3 as reactive gases. The generally high mechanical strength of silicon nitride ceramic stems from the presence of Si-N covalent bonds [6]. The quantity of Si-N bonds therefore plays a significant role in influencing the mechanical strength of silicon nitride coatings. Additionally, the temperature to which these coatings are subjected will determine the ensuing reactions [20] and, consequently, the coating's structure and properties. Therefore, the effects of ammonia (NH_3) to dichlorosilane (SiH_2Cl_2) flow ratio and deposition temperature were systemically investigated in the form of microstructure, mechanical and tribological properties of the coatings.

2. Materials and methods

2.1. Preparation of silicon nitride coatings

The silicon nitride coatings were deposited in an LPCVD system (Koyo Thermo Systems Co., Ltd, Japan) using SiH_2Cl_2 (DCS) and NH_3 gases as reactive sources. N_2 gas was used to dilute the gas mixtures to maintain the total gas flow rate. Three thermocouples were placed at the top, centre and bottom of the chamber to ensure an even and uniform heat treatment throughout the chamber. During the LPCVD deposition, three main steps were performed, including the adsorption of gas to the substrate, the chemical reaction between the gas mixtures and the desorption of gas byproducts [21].

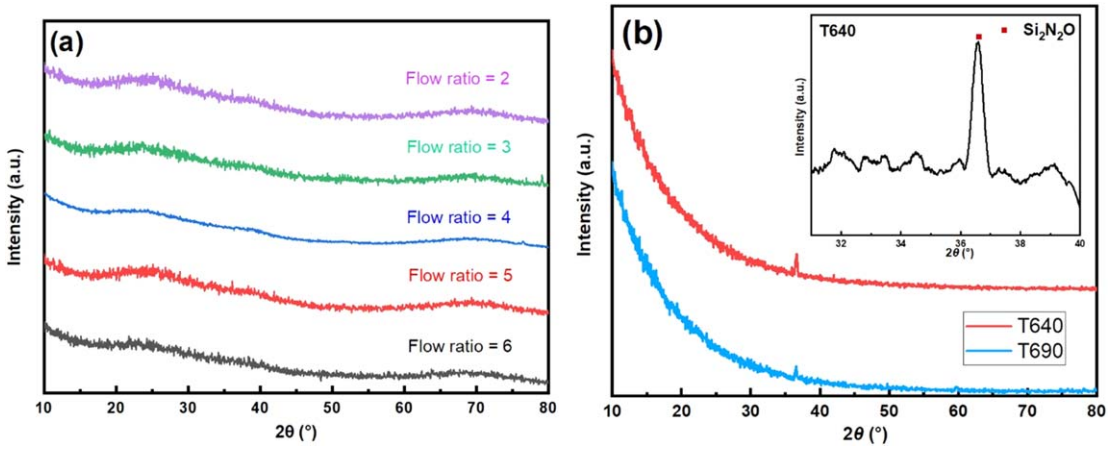

Figure 1. GI-XRD patterns of silicon nitride coatings deposited at different flow ratios (a) and temperature (b).

The coatings were deposited on (100) silicon wafers (UniversityWafer, Inc., USA). Before deposition, the substrates were cleaned ultrasonically in acetone and ethanol baths for 10 min, respectively. Then, the substrates were put in hydrofluoric acid (HF, 48% aqueous solution) bath for 1 min to remove the oxide layer on the surface. Afterwards, all samples were deposited at a chamber pressure of 220 mTorr and a deposition time of 5 h. The overall flow rate was kept at 125 sccm (cubic centimetres per minute) by adjusting the flow ratio. In order to study the influence of flow ratio and deposition temperature on the structural, mechanical and tribological properties of the silicon nitride coatings, the deposition parameters were adjusted according to the recommended standard mode of the machine (with a temperature of 790 °C, a flow rate of DCS of 25 sccm and a flow rate of NH_3 of 100 sccm). Detailed deposition parameters are shown in table 1.

2.2. Coating characterization

The phase composition of the silicon nitride coatings was analyzed by an x-ray parallel beam diffractometer (XRD, D5000 Bruker, US) with a step size of 0.02° from 10° to 80°. To analyze the top surface of the coatings, the grazing angle was set at 2°. The elemental bonding structures of the coatings were analyzed by x-ray photoelectron spectroscopy (XPS, Axis UltraDLD, Kratos Analytical, Manchester, UK) equipped with monochromatic Al ($K\alpha$) x-ray radiation. Survey scans of the samples were acquired at a pass energy of 100 eV and step size of 1 eV, and the Si2p, N1s and O1s core level spectra were obtained on an area of 1 mm^2 using transmission energy of 60 eV and step energy of 0.05 eV. The cross-sectional morphology and thickness of the coatings were investigated by scanning electron microscopy (SEM, LEO 1530 Gemini, Zeiss, Jena, Germany). The thickness was calibrated according to the inclination angle during the measurement. Meanwhile, the chemical composition was analyzed by energy-dispersive x-ray spectroscopy (EDX). The surface roughness of the sample was measured by vertical scanning interferometry (VSI, WYKO NT-110, Vecco, Germany) with a scanning area of 3×3 mm^2.

The hardness (H) and elastic modulus (E) of the coatings were measured by nanoindentation (UNHT, Anton Paar, Austria) using a diamond Berkovich tip. The elastic modulus was calculated according to Oliver-Pharr method [22]. The indentations were performed in dynamic mode with an indent depth of 10% of the coating thickness. Each sample was measured at 20 points to ensure the accuracy of the data.

2.3. Tribological testing

The coefficient of friction and wear behavior was evaluated in a ball-on-disc test under wet sliding conditions. The lubricant chosen was a simulated body fluid, composed of 25 vol.% fetal bovine serum (FBS, Gibco, EU approved, origin South America, Chicago, USA), 0.075 wt% sodium azide (Sigma-Aldrich, St. Louis, MO, USA, S8032-25G) and 20.0 mM ethylene-diaminetetraacetic acid solution (EDTA, Sigma-Aldrich, 03690) [23]. A Si_3N_4 ball (Spekuma Kullager AB, Sweden) with a diameter of 10 mm was chosen as a counterpart sliding against the samples to simulate the worse scenario and comparison with previous studies [12]. A nominal contact load of 1 N was applied, which resulted in an estimated contact pressure of 500 MPa. Typically, the contact pressure on the ceramic-on-ceramic prosthesis is around 90 MPa, but in the case of edge-loading, a maximum pressure of up to 700 MPa is reached [24]. The tests were performed for 10,000 cycles at a temperature of 37 ± 5 °C. After test completion, the wear tracks were characterized by SEM, and the wear rate was analyzed using data from VSI measurements, using Archard's equation [25].

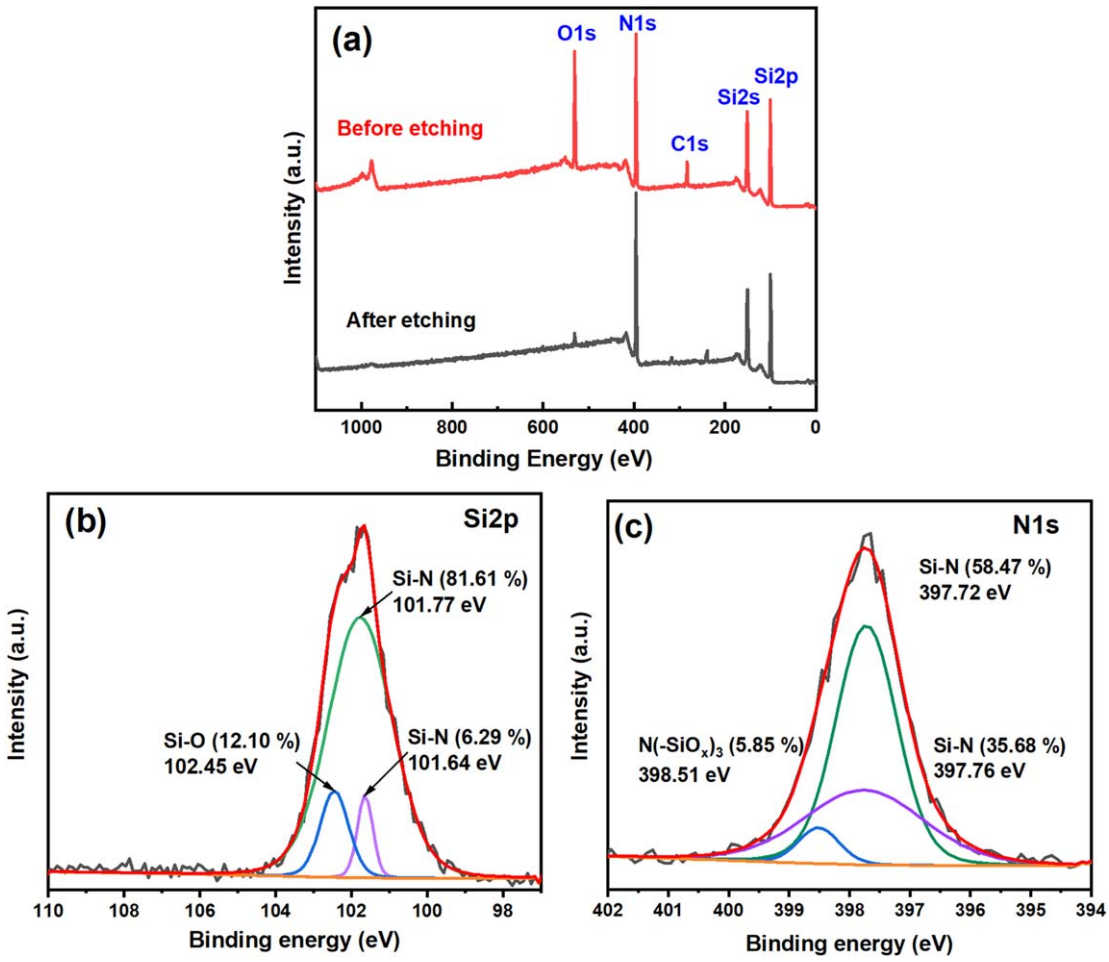

Figure 2. XPS spectra of the coatings deposited at the flow ratio of 4: (a) wide scan spectrum; (b-c) the core level spectra of Si2p and N1s.

2.4. Statistical analysis

Statistical analyses of the mechanical properties and tribological properties were carried out in the R program. A one-way ANOVA analysis followed by Tukey's HSD post-hoc test was used. A significance level of $p < 0.05$ was chosen in all analyses.

3. Results and discussion

3.1. Coating structure and composition

XRD patterns of SiNx coatings deposited at different flow ratios and temperatures are shown in figures 1(a) and (b). SiNx coatings deposited at 790 °C showed an amorphous structure, independently of the flow ratio. For the SiNx coatings deposited at lower temperatures (figure 1(b)), a weak diffraction peak was observed, assigned to the oxidation of SiNx.

In order to further investigate the chemical structure, the coating deposited at stoichiometric mode (flow ratio = 4, T = 790 °C) was analyzed by XPS, as shown in figure 2. Since XPS is a surface-sensitive technique and Si_3N_4 is easily oxidized to form a 2–5 nm thick SiO_2 layer [26, 27], the Ar ion beam was used to remove this layer. Figure 2(a) depicts the wide scan spectra of the coating, corresponding to Si, N, O, C and auger peaks. It could be seen that the intensities of the O1s peak decrease significantly after etching, indicative of surface oxidation. The core spectra of Si2p and N1s after etching are shown in figures 2(b)–(c). In order to correct the charging effect, these spectra were plotted based on the difference between the binding energy of the standard C element (284.6eV) and the binding energy of C measured from the surface [28]. The Si2p peak was centered at 101.77 eV, which is assigned to Si-N bonding while other fitting peaks corresponded to Si-O bonding. The N-Si bonds centered at 397.72 eV also contributed dominantly to N1s peak. The N(-SiOx)3 bonds centred at 398.51 eV also contributed to the N1s peak, which is attributed to nitrogen in the subnitride and true nitride local environment [29].

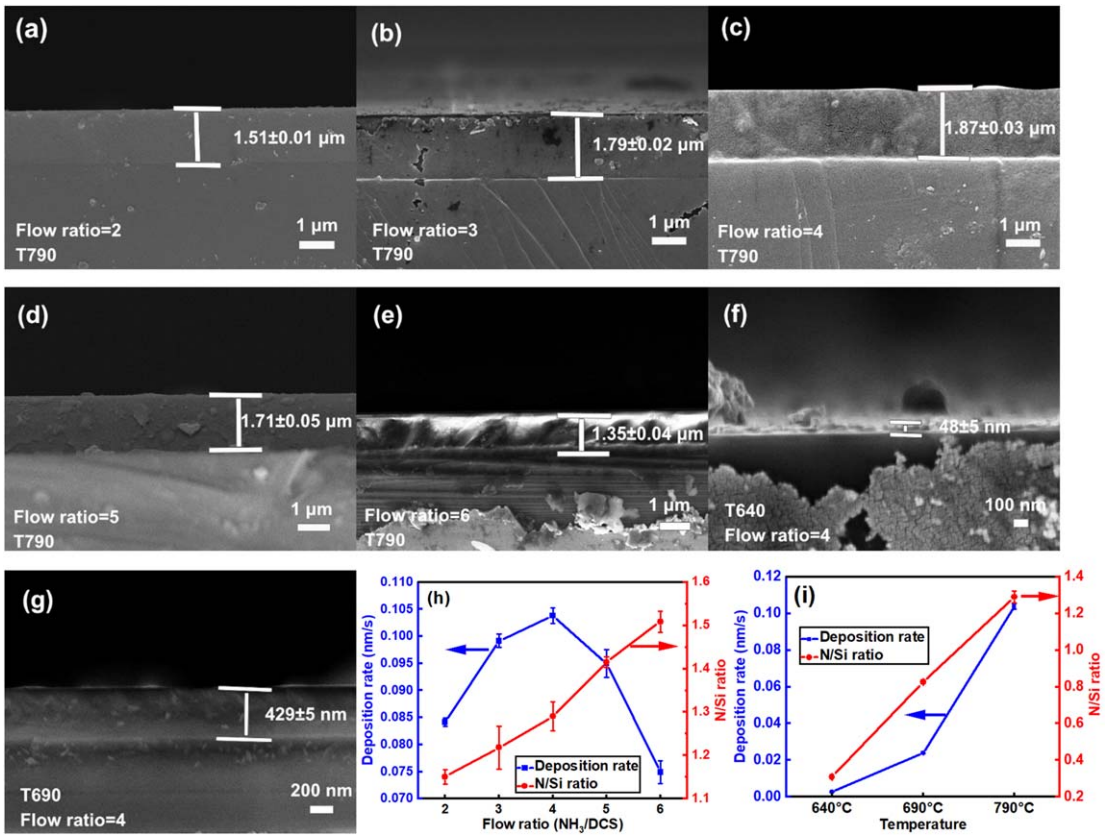

Figure 3. Cross-sectional images of the deposited coatings (a)–(g) showing the continuous and uniform interface and the thickness of the coatings; deposition rate (blue line) and N/Si ratio (red line, measured by EDX technique) as a function of flow ratio (h) and temperature (i).

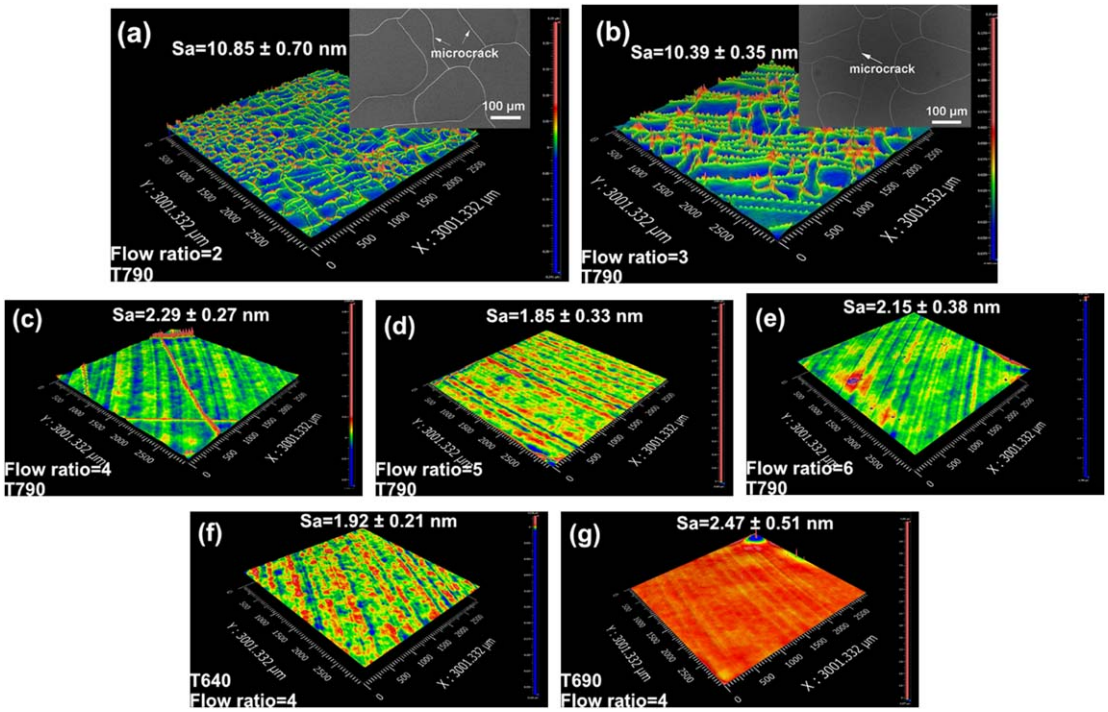

Figure 4. Typical VSI topography of the coatings measuring in an area of 3 × 3 mm^2 (a)–(g). At least three different positions were measured and the average values are indicated in the images. To further identify the microcracks of the coatings deposited by flow ratio of 2 and 3, their surface morphologies were characterized by SEM and the respective images are inserted into (a)–(b).

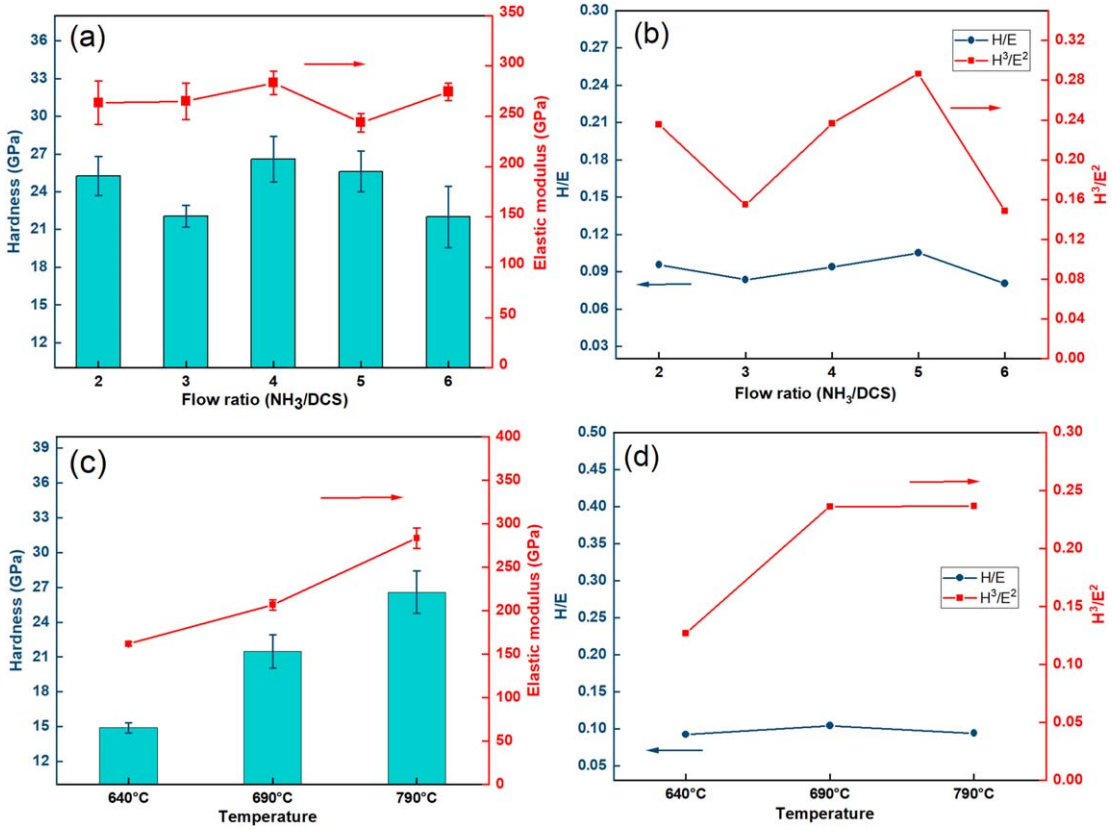

Figure 5. Mechanical properties of the silicon nitride coatings as a function of deposition flow ratio (a)(b) and temperature (c)(d). The coatings were deposited at a flow ratio of 4 when changing the temperature.

The cross-sectional morphology and thickness of the SiNx coatings deposited with different parameters were characterized by SEM, as presented in figures 3(a)–(g). The coatings displayed a dense and uniform morphology. There was a clear interface between the SiNx coating and the substrate but without any gaps, suggesting that the coatings grew continuously and uniformly. Indeed, this could be expected, as the LPCVD deposition process involves heating the chamber with thermocouples at various positions, which ensures a uniform process of mass transport and diffusion and the formation of uniform coatings [30].

The elemental composition of the coatings was analyzed by EDS, and the deposition rate was calculated by dividing the coating thickness by deposition time (5 h). The representative EDS spectra are illustrated in Supporting figure 1. Figure 3(h) illustrates the dependence of the N/Si atomic ratio and deposition rate on the flow ratio (NH_3/DCS). It could be seen that the N/Si atomic ratio increased with increasing flow ratio and reached the stoichiometric composition (Si_3N_4, N/Si = 1.33) when the flow ratio was between 4 and 5. A similar trend was reported by Liu *et al* [31]. When the NH_3 gas flow was insufficient, the DCS gas was pyrolyzed and a Si-rich SiNx coating was formed. The deposition rate also increased with an increasing flow ratio and reached a maximum at a flow ratio of 4. This trend agrees well with the Eley–Rideal mechanism [32]. During the LPCVD deposition, the NH_3 radicals were easily absorbed by the surface while DCS diffused slowly into the surface, thus the chemical reaction rate depends largely on the NH_3 flow rate.

Figure 3(i) shows the dependence of the N/Si atomic ratio and deposition rate on the deposition temperature. The N/Si atomic ratio decreased dramatically at lower temperatures. This could be due to the pyrolysis of DCS and decomposition of NH_3 at lower temperatures, and then, the Si was formed and easily oxidized in air, which is consistent with the XRD results. The deposition rate also decreased significantly with decreasing temperature in agreement with the Arrhenius mechanism [33].

The 2D morphology and 3D topography of the as-deposited coatings were characterized by SEM and VSI, respectively, as presented in figure 4. The coatings exhibited a smooth surface. The surface roughness decreased significantly with increasing flow ratio ($p < 0.05$) until reaching a minimum at a flow ratio of 5 (1.85 ± 0.33 nm). The coatings deposited at a flow ratio of 2 exhibited the highest roughness, at 10.85 ± 0.70 nm, as well as lots of peaks and valleys on the surface (figure 4(a)), which were found to be microcracks (as confirmed by SEM). According to a Monte Carlo simulation by Bouhadiche *et al*, the N content plays an important role in determining the size of Si clusters [30]. When the NH_3 gas is insufficient or the flow ratio is low, the DCS is

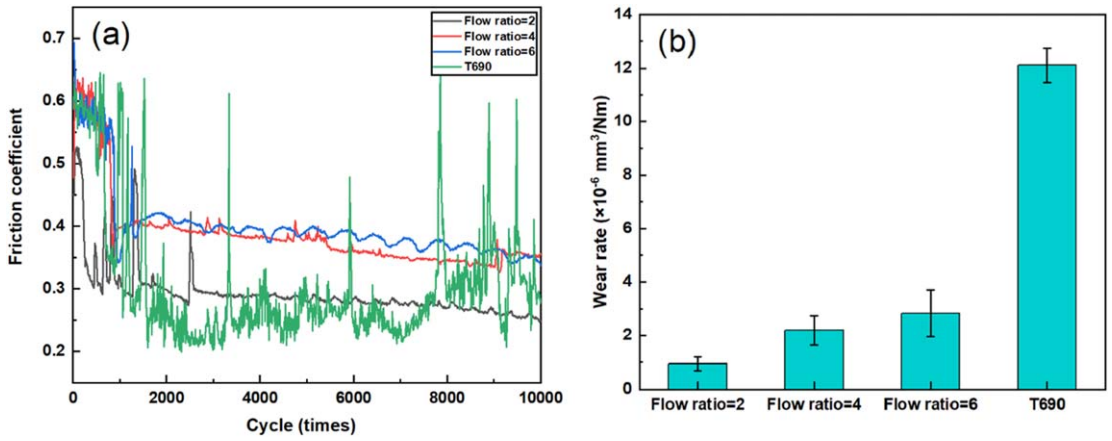

Figure 6. Dynamic friction coefficient curve (a) and the specific wear rate (b) of the coatings under the sliding cycles of 10000 and contact pressure of 500 MPa.

pyrolyzed and forms Si clusters; at a higher flow ratio, the growth and coalescence processes of Si clusters were inhibited owing to stronger Si-N bonds. Therefore, at a flow ratio of 2 and 3, large Si clusters were formed, and these clusters caused a stress mismatch and microcracks during the cooling process.

3.2. Mechanical properties of the coatings

The hardness and elastic modulus of the silicon nitride coatings deposited at different flow ratios and temperatures were characterized by nanoindentation, as presented in figure 5. The results show that the hardness (H) and elastic modulus (E) of the coatings deposited at different flow ratios ranged from 22 to 27 GPa and from 250 to 300 GPa, respectively (figure 5(a)). These values were higher than those of silicon nitride deposited using other techniques such as PECVD (with a hardness of 11–22 GPa and elastic modulus of 100–200 GPa) [34, 35], PVD (with a hardness of 9–19 GPa and elastic modulus of 118–200 GPa) [36] and rHiPIMS (with a hardness of 13–25 GPa and elastic modulus of 150–300 GPa) [23], which is most likely due to the higher density of the silicon nitride coatings deposited by the LPCVD technique [16]. Furthermore, it was observed that the hardness of the coatings increased significantly with an increasing flow ratio until it reached a maximum at a flow ratio of 4. Subsequently, it decreased with further increases in the flow ratio ($p < 0.05$). This might be related to the formation of non-stoichiometric silicon nitride coatings [35]. As confirmed by SEM-EDS (figure 3(h)), Si-rich coatings were formed when the flow ratio was less than 4, which resulted in the formation of SiO_2 clusters and correspondingly reduced the mechanical properties of the coatings. Similarly, N-rich coatings were formed when NH_3 flow was in excess, which reduces the mechanical properties due to weaker N–N bonds. The elastic modulus also significantly changed with different flow ratios ($p < 0.05$).

Figure 5(b) shows the H/E and H^3/E^2 values of the coatings deposited at different flow ratios. A rough indication of the wear resistance could be given by the H/E and H^3/E^2 ratios, since these values are key factors in determining toughness and plastic deformation, respectively [25]. Higher values indicate a better capability to resist crack growth and deformation, and thus better tribological properties. According to Musil *et al*, the hard coatings with H/E >1 showed better resistance to cracking and thus better wear resistance [37]. In this study, these H/E values were comparable to those of other bearing coatings for joint replacement such as CrN coatings (with H/E of 0.07–0.08, H^3/E^2 of 0.05–0.08) [38] and TaC coatings (with H/E of 0.085–0.113) [39]. The coatings deposited at a flow ratio of 5 showed the highest values of H/E and H^3/E^2, at 0.11 and 0.28, respectively.

Figures 5(c) and (d) present the mechanical properties of the coatings deposited at different temperatures. It could be found that the hardness and E decreased significantly with decreasing temperature ($p < 0.05$), which may be caused by the incomplete reaction between the reactive gases. Additionally, the coatings deposited at lower temperatures exhibit lower N/Si ratios (as presented in figure 3(i)), which results in poorer mechanical properties due to weaker Si-Si bonds [23].

3.3. Tribological properties of the coatings

The tribological properties were characterized by a ball-on-disc instrument, and the results for the friction coefficient and wear rate of the coatings sliding against the silicon nitride ball in the FBS solution are shown in figure 6. It could be seen that there is a run-in stage for all the coatings, which arises from the surface oxide layer. After that, the friction coefficient of the coatings deposited at different flow ratios became steady. In contrast, the friction coefficients of the coatings deposited at 690 °C were unstable during the sliding, which may be attributed

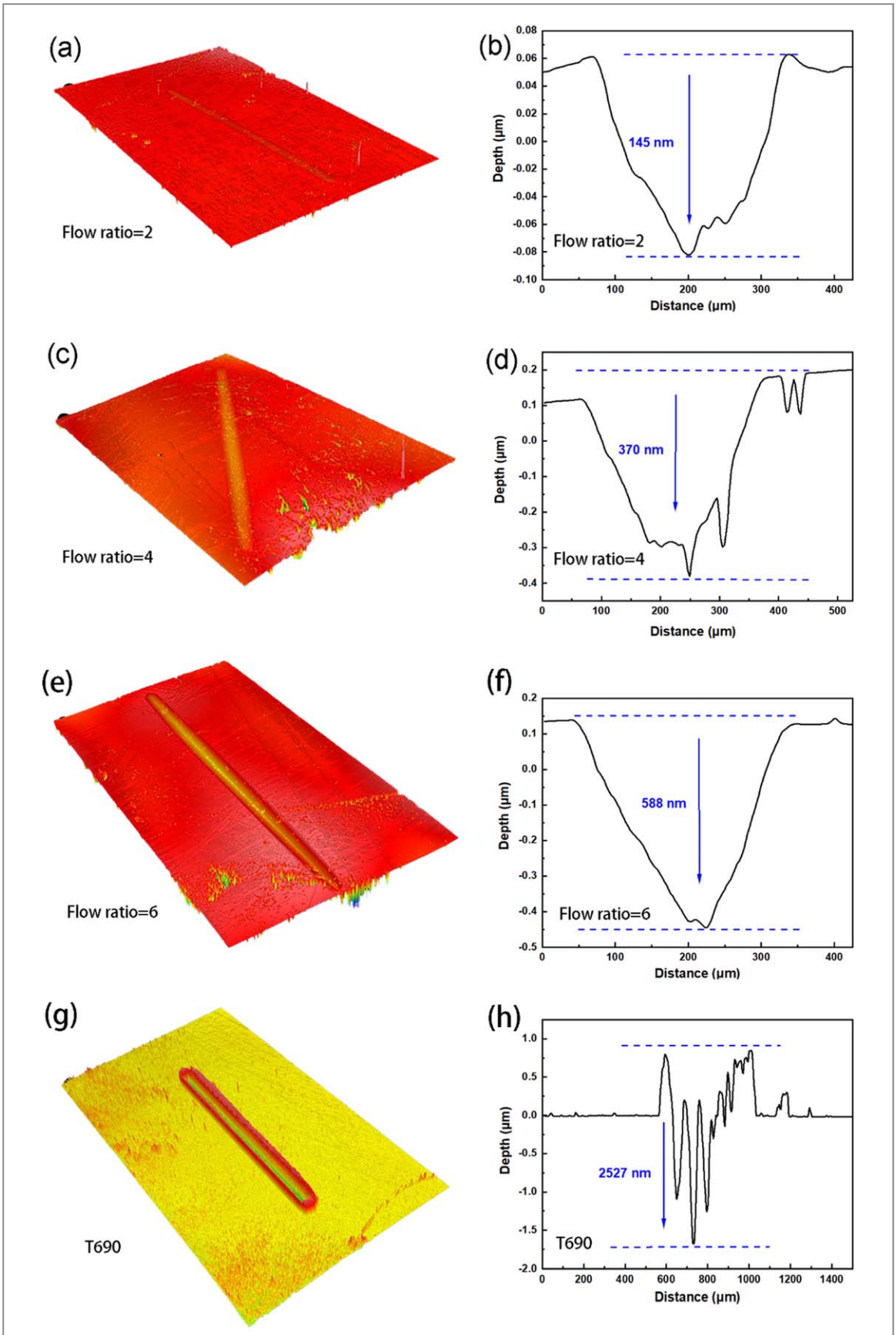

Figure 7. Three-dimensional topographies (left) and the corresponding depth profile (right) of the wear tracks of the coatings. The profiles were taken perpendicular across the wear track. Particularly, the coatings deposited at the temperature of 690 °C were worn through during the testing.

to the worse wear resistance of the coating. Thus, the counter ball wore through the coatings and created wear particles. It also showed the highest wear rate, at 12.10×10^{-6} mm^3 Nm^{-1}. The specific wear rate changes significantly at different deposition parameters ($p < 0.05$). The coating deposited at a flow ratio of 2 exhibited a lower friction coefficient (with a mean steady value of around 0.28) and the lowest wear rate (0.95×10^{-6} mm^3 Nm^{-1}). The lower friction coefficient may be due to the higher reactivity of this coating containing less N (figure 3(h)), giving rise to a lubricating layer. The higher wear rates of the coating deposited at a flow ratio of 6 may be due to this effect as well as the lower hardness of this coating (figure 5). These values were in a similar range to those of other ball-on-disc tested coatings for joint prostheses. For example, Filho *et al* obtained a friction coefficient of 0.35 and a wear rate of 0.5×10^{-5} mm^3 Nm^{-1} of silicon nitride coatings sliding against a Si_3N_4 ball under a contact pressure of 328 MPa using a rHiPIMS deposition method [12].

In order to further identify the wear mechanism of the coatings, the topographies and surface morphologies of the coatings were characterized by the VSI technique. Figure 7 shows the three-dimensional topographies and cross-sectional depth profile of the wear tracks of the coatings. It can be seen that the coatings deposited at a flow ratio of 2 exhibited the shallowest wear track, and the width and depth of the wear tracks increased with increasing flow ratio. In addition, protrusions above the coating surface can be observed, which implies that the wear mechanism is adhesive wear. The coating deposited at 690 °C shows a different wear track, with a peak-to-valley value of 2527 nm, which means that the coating delaminated during the wear testing.

4. Conclusions

LPCVD deposition of silicon nitride coatings at NH_3/DCS flow ratios between 2 and 6 and a deposition temperature of 790 °C led to amorphous, dense coatings. Lower deposition temperatures of 640 °C and 690 °C gave a diffraction peak caused by oxidation, and unstable coatings during wear tests. The thickness and deposition rate of the coatings reached maxima at a flow ratio of 4 while they increased continuously with increasing temperature (at a fixed flow ratio of 4). The roughness decreased with increasing flow ratio due to the formation of microcracks in lack of NH_3 gas flow. The hardness and elastic modulus of the coatings increased with increasing flow ratio, until reaching a maximum at the flow ratio of 4, while the friction coefficient and wear rate were the lowest at the flow ratio of 2. These results were concluded to be mainly due to the composition of the coatings, which has a significant influence on the mechanical and tribological properties.

Acknowledgments

This work was supported by the European Union's Horizon 2020 research and innovation programme under the Marie Skłodowska-Curie grant agreement No 812765. The authors are grateful to Örjan Vallin for assistance with the LPCVD machine. We acknowledge Myfab Uppsala for providing facilities and experimental support. Myfab is funded by the Swedish Research Council (2019-00207) as a national research infrastructure.

Data availability statement

All data that support the findings of this study are included within the article (and any supplementary files).

ORCID iDs

Huasi Zhou https://orcid.org/0009-0005-3234-5649

References

[1] Park S J, Lee C S, Chung S S, Lee K H, Kim W S and Lee J Y 2016 Long-term outcomes following lumbar total disc replacement using ProDisc-II *Spine (Phila Pa 1976)* **41** 971–7
[2] Sandhu F A, Dowlati E and Garica R 2020 Lumbar arthroplasty: past, present, and future *Clin. Neurosurg.* **86** 155–69
[3] Spivak J M and Petrizzo A M 2010 Revision of a lumbar disc arthroplasty following late infection *Eur. Spine. J.* **19** 677–81
[4] Reeks J and Liang H 2015 Materials and their failure mechanisms in total disc replacement *Lubricants* **3** 346–64
[5] Uwais Z A, Hussein M A, Samad M A and Al-Aqeeli N 2017 Surface modification of metallic biomaterials for better tribological properties: a review *Arab. J. Sci. Eng.* **42** 4493–512
[6] Skjöldebrand C, Tipper J L, Hatto P, Bryant M, Hall R M and Persson C 2022 Current status and future potential of wear-resistant coatings and articulating surfaces for hip and knee implants *Mater. Today Bio.* **15** 100270
[7] Amaral M, Maru M M, Rodrigues S P, Gouvêa C P, Trommer R M, Oliveira F J, Achete C A and Silva R F 2015 Extremely low wear rates in hip joint bearings coated with nanocrystalline diamond *Tribol. Int.* **89** 72–7

[8] Schmidt S, Hänninen T, Goyenola C, Wissting J, Jensen J, Hultman L, Goebbels N, Tobler M and Högberg H 2016 SiNx coatings deposited by reactive high power impulse magnetron sputtering: process parameters influencing the nitrogen content *ACS Appl. Mater. Interfaces* **8** 20385–95
[9] Pettersson M, Bryant M, Schmidt S, Engqvist H, Hall R M, Neville A and Persson C 2016 Dissolution behaviour of silicon nitride coatings for joint replacements *Mater. Sci. Eng.* C **62** 497–505
[10] Pettersson M, Skjöldebrand C, Filho L, Engqvist H and Persson C 2016 Morphology and dissolution rate of wear debris from silicon nitride coatings *ACS Biomater. Sci. Eng.* **2** 998–1004
[11] Marin E *et al* 2021 Biological responses to silicon and nitrogen-rich PVD silicon nitride coatings *Mater Today Chem.* **19** 100404
[12] Filho L, Schmidt S, Leifer K, Engqvist H, Högberg H and Persson C 2019 Towards functional silicon nitride coatings for joint replacements *Coatings* **9** 1–10
[13] Filho L C, Schmidt S, Goyenola C, Skjöldebrand C, Engqvist H, Högberg H, Toble M and Persson C 2020 The effect of N, C, Cr, and Nb content on silicon nitride coatings for joint applications *Materials* **13** 1896
[14] Filho L C, Schmidt S, López A, Cogrel M, Leifer K, Engqvist H, Högberg H and Persson C 2019 The effect of coating density on functional properties of SiNx coated implants *Materials* **12** 11–4
[15] Skjöldebrand C, Hulsart-Billström G and Engqvist H 2020 P.C. Si–Fe–C–N Coatings for biomedical applications: a combinatorial approach *Materials* **13** 2074
[16] Morin P, Raymond G, Benoit D, Maury P and Beneyton R 2012 A comparison of the mechanical stability of silicon nitride films deposited with various techniques *Appl. Surf. Sci.* **260** 69–72
[17] Jin H and Weber K J 2007 The effect of low pressure chemical vapor deposition of silicon nitride on the electronic interface properties of oxidized silicon wafers *Prog. Photovoltaics Res. Appl.* **15** 405–14
[18] Cossou B, Jacques S, Couégnat G, King S W, Li L, Lanford W A, Bhattarai G, Paquette M and Chollon G 2019 Synthesis and optimization of low-pressure chemical vapor deposition-silicon nitride coatings deposited from SiHCl 3 and NH 3 *Thin Solid Films* **681** 47–57
[19] Roenigk K F and Jensen K F 1987 Low pressure CVDof silicon nitride *J. Electrochem. Soc.* **134** 1777
[20] Cossou B, Jacques S, Couégnat G, King S W, Li L, Lanford W A, Bhattarai G, Paquette M and Chollon G 2019 Synthesis and optimization of low-pressure chemical vapor deposition-silicon nitride coatings deposited from SiHCl 3 and NH 3 *Thin Solid Films* **681** 47–57
[21] Tonnberg S 2006 *Optimisation and characterisation of LPCVD Silicon Nitride Thin Film Growth* Chalmers University of Technology 62
[22] Pharr G M and Oliver W C 1992 Measurement of thin film mechanical properties using nanoindentation *MRS Bull.* **17** 28–33
[23] Skjöldebrand C, Schmidt S, Vuong V, Pettersson M, Grandfield K, Högberg H, Engqvist H and Persson C 2017 Influence of substrate heating and nitrogen flow on the composition, morphological and mechanical properties of SiNx coatings aimed for joint replacements *Materials* **10** 1–11
[24] Sanders A P and Brannon R M 2011 Assessment of the applicability of the hertzian contact theory to edge-loaded prosthetic hip bearings *J. Biomech.* **44** 2802–8
[25] Yan M, Wang X, Zhou H, Liu J, Zhang S, Lu Y and Hao J 2021 Microstructure, mechanical and tribological properties of graphite-like carbon coatings doped with tantalum *Appl. Surf. Sci.* **542** 148404
[26] Ermakova E, Rumyantsev Y, Shugurov A, Panin A and Kosinova M 2015 PECVD synthesis, optical and mechanical properties of silicon carbonnitride films *Appl. Surf. Sci.* **339** 102–8
[27] Bal B S and Rahaman M N 2012 Orthopedic applications of silicon nitride ceramics *Acta Biomater.* **8** 2889–98
[28] Vassallo E, Cremona A, Ghezzi F, Dellera F, Laguardia L, Ambrosone G and Coscia U 2006 Structural and optical properties of amorphous hydrogenated silicon carbonitride films produced by PECVD *Appl. Surf. Sci.* **252** 7993–8000
[29] Matsuoka M, Isotani S, Sucasaire W, Zambom L S and Ogata K 2010 Chemical bonding and composition of silicon nitride films prepared by inductively coupled plasma chemical vapor deposition *Surf. Coat. Technol.* **204** 2923–7
[30] Bouhadiche A, Bouridah H and Boutaoui N 2014 Kinetic monte carlo simulation of low-pressure chemical vapor deposition of silicon nitride: impact of gas flow rate and temperature on silicon cluster size and density *Mater. Sci. Semicond. Process.* **26** 555–60
[31] Liu X J, Zhang J J, Sun X W, Pan Y B, Huang L P and Jin C Y 2004 Growth and properties of silicon nitride films prepared by low pressure chemical vapor deposition using trichlorosilane and ammonia *Thin Solid Films* **460** 72–7
[32] Zhang S L, Wang J T, Kaplan W and Östling M 1992 Silicon nitride films deposited from SiH2Cl2-NH3 by low pressure chemical vapor deposition: kinetics, thermodynamics, composition and structure *Thin Solid Films* **213** 182–91
[33] Xiang D, Xia H, Yang W and Mou P 2019 Parametric study and residual gas analysis of large-area silicon-nitride thin-film deposition by plasma-enhanced chemical vapor deposition *Vacuum* **165** 172–8
[34] Huang H, Winchester K J, Suvorova A, Lawn B R, Liu Y, Hu X Z, Dell J M and Faraone L 2006 Effect of deposition conditions on mechanical properties of low-temperature PECVD silicon nitride films *Mater. Sci. Eng.* A **435** 453–9
[35] Zhou H, Persson C, Xia W and Engqvist H 2023 SiNx coating deposition on cocr by plasma-enhanced chemical vapor deposition *Biomedical Materials & Devices* 1–8
[36] Rao A U, Tiwari S K, Goyat M S and Chawla A K 2023 Recent developments in magnetron-sputtered silicon nitride coatings of improved mechanical and tribological properties for extreme situations *J. Mater. Sci.* **58** 9755–804
[37] Musil J 2012 Hard nanocomposite coatings: thermal stability, oxidation resistance and toughness *Surf. Coat. Technol.* **207** 50–65
[38] Xu X, Sun J, Xu Z, Li Z and Su F 2021 Microstructure, electrochemical and tribocorrosion behaviors of CrCN nanocomposite coating with various carbon content *Surf. Coat. Technol.* **411** 126997
[39] Du S, Zhang K, Wen M, Qin Y, Li R, Jin H, Bao X, Ren P and Zheng W 2018 Optimizing the tribological behavior of tantalum carbide coating for the bearing in total hip joint replacement *Vacuum* **150** 222–31